Infrared Physics & Technology 52 (2009) 344–347

Contents lists available at ScienceDirect

Infrared Physics & Technology

journal homepage: www.elsevier.com/locate/infrared

InAs/GaSb superlattices for advanced infrared focal plane arrays

Robert Rehm [a,*], Martin Walther [a], Johannes Schmitz [a], Frank Rutz [a], Joachim Fleißner [a], Ralf Scheibner [b], Johann Ziegler [b]

[a] Fraunhofer-Institut für Angewandte Festkörperphysik, Tullastr. 72, Freiburg 79108, Germany
[b] AIM Infrarot-Module GmbH, Theresienstr. 2, Heilbronn 74072, Germany

ARTICLE INFO

Article history:
Received 11 September 2009
Available online 19 September 2009

PACS:
07.57.Kp
85.60.Gz
95.85.Hp

Keywords:
InAs/GaSb superlattice
Quantum efficiency
Infrared focal plane array
MWIR
Dual-color
Carbon dioxide

ABSTRACT

We report on the development of high performance focal plane arrays for the mid-wavelength infrared spectral range from 3–5 μm (MWIR) on the basis of InAs/GaSb superlattice photodiodes. An investigation on the minority electron diffusion length with a set of six sample ranging from 190 to 1000 superlattice periods confirms that InAs/GaSb superlattice focal plane arrays achieve very high external quantum efficiency. This enabled the fabrication of a range of monospectral MWIR imagers with high spatial and excellent thermal resolution at short integration times. Furthermore, novel dual-color imagers have been developed, which offer advanced functionality due to a simultaneous, pixel-registered detection of two separate spectral channels in the MWIR.

1. Introduction

Proposed in 1987 by Smith and Mailhiot, short-period InAs/GaSb superlattices (SLs) represent a very attractive quantum system for high performance infrared (IR) detectors [1]. The two materials form a broken gap type-II system, where the conduction band edge of InAs is lower in energy than the GaSb valence band edge. When both constituent's individual layer thickness is thin, an artificial band gap results on the basis of spatially separated electron and hole states in the InAs and GaSb layers, respectively. The effective band gap can be adjusted from approximately 3–30 μm by altering layer thickness, which can be precisely and homogeneously controlled during molecular beam epitaxy (MBE). Typical values for the layer thickness of both materials in a single SL period range from 5–15 monolayers (ML) each. The coupling of neighboring electron wave functions leads to the formation of an electron miniband. Holes, however, are strongly localized within the GaSb layers, which drastically reduces their mobility along the growth axis. The electron effective mass is significantly larger than in $Cd_xHg_{1-x}Te$ (CMT) and depends only weakly on the effective band gap. Tunneling contributions to the dark current are therefore reduced. The valence band structure can be adjusted such that non-radiative auger recombination can be significantly reduced in p-type material. The long lifetime of minority electrons, good vertical carrier mobility and a high absorption coefficient result in an efficient conversion of incident IR photons into an external electrical signal current.

On the basis of the artificial band gap in InAs/GaSb SLs IR-photodiodes are realized by employing an appropriate doping profile along the SL growth axis. The built-in electric field separates photogenerated carriers even without an externally applied bias voltage and thus minimizes the power consumption. The active area is sandwiched between ohmic n- and p-type contacts comprised of an appropriate combination of doped semiconductor material and a metallization sequence. InAs/GaSb SL photodiodes show broad-band absorption characteristics, where the long-wavelength cut-off is determined by the SL band gap and the short-wavelength cut-on is usually given by the spectral characteristics of the optical entrance window. Since these devices present the integrated signal of a single wave band they are referred to as monospectral detectors.

Under photovoltaic operation two independent sources contribute to the noise in a photodiode. The random thermal motion of charge carriers causes Johnson noise $J_n^2 = 4k_BT/(R_0A)$. Additionally, the incident background photon flux gives rise to shot noise

* Corresponding author. Tel.: +49 761 5159 353; fax: +49 761 5159 400.
E-mail address: Robert.Rehm@iaf.fraunhofer.de (R. Rehm).

1350-4495/$ - see front matter © 2009 Elsevier B.V. All rights reserved.
doi:10.1016/j.infrared.2009.09.005

$J_n^2 = 2e^2\eta\Phi_B$. In the above expressions k_B is the Boltzmann constant, T denotes the temperature, R_0A is the differential dark resistance area product at zero bias voltage, e symbolizes the electronic charge, η represents the quantum efficiency and Φ_B indicates the background photon flux density. In most application Φ_B is fairly stable and mostly determined by the average scene temperature and the chosen *f*-number of the camera optics. The background induced shot noise sets a lower limit to the detector performance. Thus, when $R_0A \gg 2k_BT/(e^2\eta\Phi_B)$ the detector operates with background-limited performance (BLIP) and the detectivity, i.e., the normalized signal-to-noise ratio, is then given by the well known expression

$$D^*_{BLIP} = \frac{\lambda}{hc}\sqrt{\frac{\eta}{2\Phi_B}}. \quad (1)$$

Accordingly, under background-limited operation the detectivity is improved by increasing the quantum efficiency. While a further increase of the R_0A product would allow to raise the operation temperature of the detector, no detection performance can be gained by an additional reduction of the dark current once BLIP conditions have been reached.

InAs/GaSb SL photodiodes in the mid-wavelength IR spectral range (3–5 μm, MWIR) with a cut-off wavelength around 5 μm reveal a R_0A product beyond $10^5\ \Omega\,\mathrm{cm}^2$ at 77 K. For a 300 K scene background-limited performance is achieved with conventionally used f-numbers.

2. Quantum efficiency of InAs/GaSb superlattice photodiodes

The quantum efficiency η depends on the reflection losses R at the photodiode surface, the absorption coefficient α, the electron diffusion length L_e in growth direction, the thickness of the depletion region d_{DR}, and the thickness of the neutral n- and p-regions, d_n and d_p, respectively. Due to their low mobility the contribution of minority holes to the quantum efficiency in InAs/GaSb photodiodes can be neglected. According to Ref. [2], for front side illuminated n-on-p photodiodes, η is then given by

$$\eta = (1-R)e^{-\alpha d_n}\left[(1-e^{-\alpha d_{DR}}) + \frac{\alpha L_e}{\alpha^2 L_e^2 - 1}e^{-\alpha d_{DR}}\left(\frac{-\alpha L_e e^{-\alpha d_p} - \sinh\left(\frac{d_p}{L_e}\right)}{\cosh\left(\frac{d_p}{L_e}\right)} + \alpha L_e\right)\right]. \quad (2)$$

The quantum efficiency increases proportionally with the absorber thickness, but saturates once the absorber thickness and the electron diffusion length become comparable. Provided that the electron diffusion length is sufficiently large, even for a modest α an increase of the absorber layer thickness allows a theoretical quantum efficiency close to unity. However, raising the absorber layer thickness beyond the diffusion length increases the diffusion contribution to the dark current without improving the quantum efficiency, since the photogenerated minority electrons recombine before reaching the space charge region [2].

To investigate the electron diffusion length in growth direction in MWIR InAs/GaSb SL photodiodes a set of six samples with increasing absorber layer thickness were grown by MBE on nominally undoped 2 in. (100) GaSb substrates. Investigations on lateral carrier diffusion can be found in Ref. [3]. On top of a 500 nm AlGaAsSb lattice matched buffer layer, 1500 nm of GaSb:Be ($1 \times 10^{18}\ \mathrm{cm}^{-3}$) were followed by the active SL region terminated by 20 nm of InAs:Si ($5 \times 10^{17}\ \mathrm{cm}^{-3}$). Each period of the active SL was composed of 10 ML InAs/10 ML GaSb resulting in a 50% cut-off wavelength of roughly 5.0 μm. The average length of a period determined by high-resolution X-ray diffraction was $p = 6.31$ nm. The active region consists of $N_p = 40$ p-type InAs/GaSb:Be ($1 \times 10^{17}\ \mathrm{cm}^{-3}$) periods, followed by $N_{n.i.d.}$ not intentionally doped, residually p-type InAs/GaSb periods and topped by $N_n = 60$ n-type InAs:Si/GaSb ($5 \times 10^{17}\ \mathrm{cm}^{-3}$) periods. For the six samples the chosen number $N_{n.i.d.}$ of periods in the n.i.d. layer were 90, 270, 405, 540, 720 and 900, respectively.

Following from Eq. (2), Fig. 1 shows the expected dependence of the single optical pass quantum efficiency on the number of p-type absorber periods $N_{n.i.d.} + N_p$ for various values of the electron diffusion length L_e assuming no reflection losses at the photodiode surface ($R = 0$) and $\alpha = 4000\ \mathrm{cm}^{-1}$. Please note, that in the vertical photodiode design chosen for the above set of samples, the maximum achievable quantum efficiency is about 0.86 due to optical absorption losses within the upper 60 n-type SL periods, in which the minority holes do not contribute to the responsivity. In Fig. 1 this threshold is indicated by a solid line labeled "Maximum".

Following MBE growth, each of the six wafers was cleaved into quarters. One quarter per wafer was used to determine the absorption coefficient α of that particular SL photodiode by Fourier-transform infrared transmission spectroscopy. Free carrier absorption in the substrate and in the 1500 nm GaSb:Be has been taken into account. On a second quarter per wafer, mesa photodiodes were dry chemically etched, dielectrically passivated and metallized. In order to illuminate the diodes from the front side, a mask set with devices featuring an optical window in the top n-contact metallization was used.

The responsivity $\propto\eta$ at 77 K measured with a Fourier-transform spectrometer is shown in Fig. 2 in arbitrary units. The signature around 4.3 μm is due to carbon dioxide absorption. Up to an absorber thickness of 940 periods no saturation of the responsivity is observed.

For each sample experimental photoresponse data shown in Fig. 2 have been extracted at the wavelength corresponding to $\alpha = 4000\ \mathrm{cm}^{-1}$. The dots in Fig. 1 show a fit of this data set to the theoretical curves. The experimentally observed photoresponse shows the theoretically expected dependence on absorber thickness when a diffusion length much beyond 940 periods (corresponding to roughly 6 μm) is assumed. In fact, the significant rise of the photoresponse between 760 and 940 periods is clear evidence of a diffusion length much larger than the absorber layer thickness of the thickest sample in this experiment.

Similar results on the diffusion length and quantum efficiency in long-wavelength infrared InAs/GaSb SL photodiodes with a 50% cut-off around 11 μm have been published by Nguyen et al. [4].

In a standard backside illuminated focal plane array (FPA) configuration the top contact metallization of each photodiode acts as

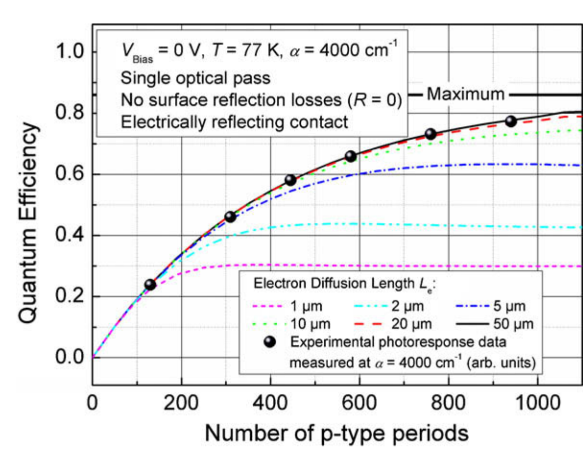

Fig. 1. Theoretical dependence of the quantum efficiency on the number of p-type absorber periods for different values of the electron diffusion length. The dots show a fit of experimental data extracted from Fig. 2 (see text for details).